situation: (i) In our attempt to enhance z, the number of magnetic neighbors, we were only partially successful (in **2**, z = 16/3, larger than z = 4 in **1** but less than z = 6 in the expected ideal structure); or (ii) the nonnegligible presence of low-spin Cr^{II} (0.175) in the $B(CN)_6$ sites induces a structural (and magnetic) disorder, which defeats our experimental strategy. The exchange interaction in **2** is therefore more complex than in **1**, and its detailed description would be beyond the scope of this note. It can be said, however, that the lowering of T_C in **2**, compared with **1**, is in large part a result of the fact that two t_{2g} unpaired electrons of the low-spin Cr^{II} present in **2** are less efficient in inducing antiferromagnetic interactions than the three of Cr^{III} in **1**.

An important property of the two compounds is their stability in atmospheric conditions: They may be left for weeks in the laboratory in bottles opened to air from time to time without apparent chemical change of Cr^{II} or loss of the magnetic properties. Such stability is surprising (the reduction properties of Cr^{II} are well-known) but valuable because it opens the possibility of useful applications at room atmosphere. The two compounds, stirred in hydrochloric acid (1 mol liter^{-1}) for 24 hours and then dried under vacuum at 100°C, remain unchanged on return to room atmosphere. In both compounds, the μ-cyano Cr^{III}-Cr^{II} insoluble network, as soon as it is formed, appears robust and chemically inert.

The deep green compound **2** deserves further comment: It displays in the near IR, in contrast to the light gray **1**, an intense absorption band centered at 8720 cm^{-1}, a much lower energy than that of the intervalence band of Prussian blue (15,000 cm^{-1}) (*34*). Hence, **2** presents a higher T_C (190 K compared with 5.5 K) and an easier electronic delocalization than Prussian blue. These two associated properties can open new perspectives in the field, and we consider **2** as the first member of a series of promising new systems.

We are now engaged in a more complete characterization of the two compounds and, in particular, in the study of their magneto-optical properties. Growth of single crystals and new syntheses are in progress in order to obtain new bimetallic and mixed-valence systems with higher T_C.

REFERENCES AND NOTES

1. O. Kahn, *Molecular Magnetic Materials*, D. Gatteschi, O. Kahn, J. S. Miller, F. Palacio, Eds. (NATO Advanced Study Institutes Series, Ser. E, Kluwer, Dordrecht, Netherlands 1991), vol. 198, pp. 35–52; J. S. Miller, *ibid.*, pp. 151–158; P. Rey, *ibid.*, pp. 203–214; A. Caneschi, *ibid.*, pp. 215–232; V. Gadet, *ibid.*, pp. 281–295.
2. J. M. Manriquez *et al.*, *Science* **252**, 1415 (1991).
3. W. D. Griebler and D. Babel, *Z. Naturforsch. Teil B* **87**, 832 (1982).
4. P.-M. Allemand *et al.*, *Science* **253**, 301 (1991).
5. M. Woodward, *Philos. Trans. R. Soc. London* **33**, 15 (1734).
6. B. N. Figgis and J. Lewis, in *Progress in Inorganic Chemistry*, F. A. Cotton, Ed. (Wiley-Interscience, New York, 1964), vol. 6, p. 188.
7. H. U. Gudel, H. Stucki, A. Lúdi, *Inorg. Chim. Acta* **7**, 121 (1973).
8. A. Lüdi and H. U. Güdel, in *Structure and Bonding* J. D. Dunitz *et al.*, Eds. (Springer-Verlag, Berlin, 1973), vol. 14, pp. 1–21.
9. The k/ℓ ratio depends on the charges of A and B; when $k/\ell > 1$, $B(CN)_6$ vacancies occur and are filled by water molecules. For B^{III} and A^{II}, the formula is $A^{II}_{\cdots}[B^{III}(CN)_6]_{\cdots}\cdot nH_2O$; k/ℓ = 3/2, and 1/3 of the $B(CN)_6$ positions are vacant. A has a mean of z = 4 B neighbors. Insertion of Cs^{I} in half of the tetrahedral sites of the network suppresses the vacancies and leads to a 1/1 stoichiometry: $Cs^{I}[A^{II}B^{III}(CN)_6]\cdot nH_2O$, A now having z = 6 B neighbors.
10. A. N. Holden *et al.*, *Phys. Rev.* **102**, 1463 (1956).
11. R. M. Bozorth *et al.*, *ibid.* **103**, 572 (1956).
12. A. Ito, M. Suenaga, K. Ono, *J. Chem. Phys.* **48**, 3597 (1968).
13. The results of such an analysis in 3D ferrimagnets, done with mean field theory and neglect of direct interaction between next-nearest neighbors (*14*), lead to $T_C = z|J|\sqrt{(C_A C_B)}/N_A g^2 \mu_B^2$, where z is the number of nearest magnetic neighbors, C_A and C_B are Curie constants, g is the mean g factor for A and B, and μ_B is the Bohr magneton.
14. L. Néel, *Ann. Phys. Paris* **3**, 10 (1948).
15. The spin delocalization on the cyanide ion was experimentally demonstrated by spin-polarized neutron studies (*16*).
16. B. N. Figgis, J. B. Forsyth, P. A. Reynolds, *Inorg. Chem.* **26**, 101 (1989).
17. Such a treatment is available through various models of exchange interaction (*18–21*) that define differently the wave functions $|a\rangle$ and $|b\rangle$ describing the unpaired electrons 1 and 2 on centers A and B. Different but equivalent expressions of J are therefore available. It is convenient to consider J as the sum of the different orbital interactions (or exchange pathways) J_{ab}, themselves split into antiferromagnetic [J_{ab}(AF) < 0] and ferromagnetic [J_{ab}(F) > 0] terms
$$J \propto \sum_{a,b} J_{ab} \propto \sum_{a,b} J_{ab}(F) + J_{ab}(AF)$$
$$= J(F) + J(AF)$$
In a model of localized electrons (*21*), J_{ab}(F) is related to the bielectronic exchange integral $j = \langle a(1)\, b(2) \,|e^2/r_{12}|\, a(2)\, b(1)\rangle$: $J_{ab}(F) \propto j$ and J_{ab}(AF) is related to the monoelectronic overlap integral $S = \langle a(1) \mid b(1)\rangle$: $J_{ab}(AF) \propto S^2$.
18. P. W. Anderson, in *Magnetism*, G. T. Rado and H. Suhl, Eds. (Academic Press, New York, 1963), vol. 1, p. 25.
19. J. B. Goodenough, *Magnetism and the Chemical Bond* (Wiley, New York, 1963).
20. P. J. Haÿ, J. C. Thiebault, R. Hoffmann, *J. Am. Chem. Soc.* **97**, 4884 (1975).
21. O. Kahn, in *Magneto-Structural Correlations, in Exchanged Coupled Systems*, D. Gatteschi, O. Kahn, R. D. Willett, Eds. (Reidel, Dordrecht, Netherlands, 1985), p. 37.
22. All the antiferromagnetic terms are zero and six t_{2g}-e_g ferromagnetic exchange pathways are present: $J \propto \Sigma_{e_g,t_{2g}} J_{ab}(F) = J_F > 0$.
23. V. Gadet, thesis, Université Pierre et Marie Curie, Paris (1992).
24. ———, T. Mallah, I. Castro, P. Veillet, M. Verdaguer, *J. Am. Chem. Soc.* **114**, 9213 (1992).
25. It has been proposed (*21, 26*) that when the energies of a and b orbitals are different, as in Figure 2B, $J_{ab}(AF) \propto S\sqrt{(\Delta^2 - \delta^2)}$, where Δ and δ are defined in Fig. 2B. Most often, when $S \neq 0$, $|J_{ab}(AF)| > J_{ab}(F)$.
26. P. Tola, O. Kahn, C. Chauvel, H. Coudanne, *Nouv. J. Chim.* **1**, 467 (1977).
27. The same compound, **1**, is obtained from the reaction of solutions of $K_4[Cr^{II}(CN)_6]$ with $Cr^{III}Cl_3$, under similar conditions. The unit cell formula of **1** is $\{Cr_4^{II}\,[Cr^{III}(CN)_6]_{8/3}[\ ]_{4/3}\cdot(H_2O)_{40/3}$, where [ ] stands for $[B(CN)_6]$ vacancies.
28. K. Nakamoto, *Infrared and Raman Spectra of Inorganic and Coordination Compounds* (Wiley, New York, ed. 3, 1978), pp. 259–267.
29. Assuming a mean g = 2 value for Cr^{III} and Cr^{II} ions and $N_A \mu_B^2/3k$ = 1/8.
30. No appreciable change was observed during operation at T = 2 K.
31. Traces of potassium and chlorine (<0.3%) appear in some preparations, without significant change of the magnetic properties. The unit cell formula of **2** is $Cs_{8/3}\{Cr_4^{II}\ Cr_{32/9}^{III}\ (CN)_{192/9}\ [\ ]_{4/9}\cdot(H_2O)_{160/9}$, where [ ] stands for $[B(CN)_6]$ vacancies.
32. J. P. Eaton and D. Nicholls, *Transition Met. Chem.* **6**, 203 (1981).
33. We plan to check the assumption of an intervalence band by examining the electronic spectra at low temperature.
34. M. B. Robin, *Inorg. Chem.* **1**, 337 (1962).

35. We acknowledge I. Castro, M. Delamare, F. Hardouin, C. Hélary, Y. Journaux, C. Mathonnière, and F. Robert for their help in the experimental studies.

12 July 1993; accepted 20 September 1993

Binding to DNA and the Retinoblastoma Gene Product Promoted by Complex Formation of Different E2F Family Members

Wilhelm Krek, David M. Livingston,* Suman Shirodkar

The E2F family of transcription factors functions in the control of the mammalian cell cycle. Here it is shown that two family members, E2F-1 and DP-1, form specific heterodimers in vivo, a process that enhances DNA binding, transactivation, and the binding of the retinoblastoma gene product. These results suggest that heterodimerization regulates E2F function and contributes to cell cycle control.

The E2F family of transcription factors (*1*) contributes to cell cycle regulation through the controlled activation of certain growth-responsive genes (*2*). Complementary DNAs (cDNAs) from two family members, E2F-1 and DP-1, were cloned and shown to be components of Rb-E2F complexes (*3–6*). Because E2F can bind its cognate DNA binding motif as a complex of different subunits in vitro (*7*), we examined whether

Dana-Farber Cancer Institute and Harvard Medical School, Boston, MA 02115.

*To whom correspondence should be addressed.

E2F-1 and DP-1 form heterodimers in vitro and in vivo.

In vitro–translated E2F-1, tagged with the influenza hamagglutinin epitope (HA), was mixed with the DP-1 translation product and subjected to immunoprecipitation with HA monoclonal antibody (mAb). DP-1 was not immunoprecipitated by HA mAb (Fig. 1A). When HA–E2F-1 and DP-1 were mixed, the same antibody precipitated both DP-1 and HA–E2F-1 (Fig. 1A), suggesting that complexes had formed. Similar results were obtained when only DP-1 was epitope tagged (*8*).

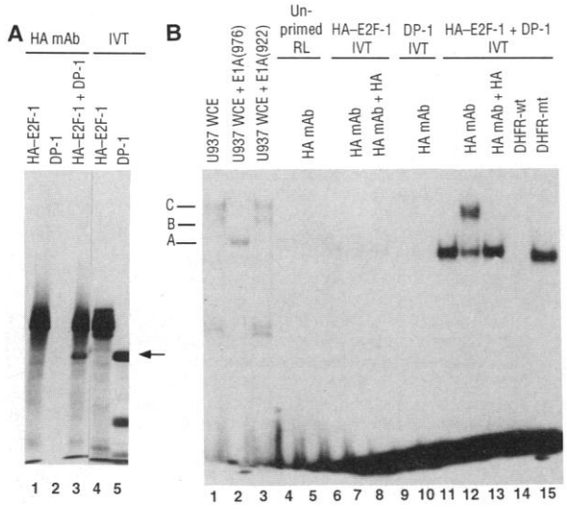

Fig. 1. E2F-1 and DP-1 associate in vitro and stimulate E2F-specific DNA binding activity. (**A**) HA–E2F-1 and DP-1 (*22*) were translated in vitro and subjected to HA mAb immunoprecipitation either alone (lanes 1 and 2) or after mixing (lane 3) (*23*). In vitro translation (IVT) products of HA–E2F-1 and DP-1 (indicated by an arrow) are shown in lanes 4 and 5, respectively. (**B**) IVT products of E2F-1 and DP-1 were incubated with an E2F oligonucleotide, either singly or after mixing, and analyzed by EMSA (*24*). Lanes 1 through 3 reveal E2F complexes in U937 cells (lane 1) and the effects of GST-E1A wild type (976) (lane 2) and GST-E1A mutant (922) (lane 3) on them. Side markers: A, free E2F; B, Rb-E2F complexes; C, E2F-p107-cyclin A-cdk2 complexes. HA mAb supershifting in the absence (lanes 7 and 12) or presence of HA peptide (lanes 8 and 13). Competition experiments were done with oligonucleotides containing either a wild-type (wt, lane 14) or a mutant (mt, lane 15) E2F site derived from the dihydrofolate reductase (DHFR) promoter (*9*). RL, reticulocyte lysate; WCE, whole-cell extracts.

In vitro–translated HA–E2F-1 displayed marginal E2F DNA binding activity, whereas DP-1 showed none (Fig. 1B). By contrast, mixing both increased the sequence-specific DNA binding activity of the former (Fig. 1B). These data suggest that DP-1 and E2F-1 form stable complexes and that complex formation is a prerequisite for high DNA binding activity. These complexes were incompletely supershifted by HA mAb (Fig. 1B). Presumably, in some of them, the HA tag is either cleaved off or sterically hindered.

In the E2F-1 sequence is a short basic region (b), two helical segments separated by a short nonhelical stretch (H1-H2), and a hydrophobic heptad repeat (Zip) (Fig. 2A). To identify regions of E2F-1 that are required for DP-1 binding, we mixed and assayed in vitro translates of the relevant polypeptides for DNA binding activity. The b–H1-H2–Zip segment (Fig. 2B), but not b–H1-H2 (Fig. 2C), bound to HA–DP-1 (complex A). Thus, heterodimerization of E2F-1 and DP-1 requires the E2F-1 zipper. The b–H1-H2–Zip and the b–H1-H2 segment are able to form homooligomers, which are probably dimers (complex B in Fig. 2B and complex C in Fig. 2C), as indicated by the appearance of a gel shift complex (Y) when HA–E2F-1 and b–H1-H2 are mixed (Fig. 2D). These data suggest that the minimal unit required for homodimerization is the b–H1-H2 segment. Similarly, the b–H1-H2–Zip and b–H1-H2 products, when mixed, also formed homodimers (complex Z, Fig. 2D). Neither the H1-H2–Zip nor the H1-H2 products bound DNA or DP-1 (*8*), suggesting that the basic region is potentially involved in DNA binding or oligomerization or both.

The in vivo association of E2F-1 and DP-1 was tested with mammalian expression plasmids encoding E2F-1 and DP-1 (tagged and untagged) introduced into the Rb (−/−) cell line, Saos-2. Transfection of HA–E2F-1 DNA led to two weak DNA binding complexes, which were absent in untransfected cell extracts (Fig. 3A). No new DNA binding complexes were detected in extracts of cells transfected with HA–DP-1 (Fig. 3A). However, cotransfection of E2F-1 and DP-1 resulted in an increase in the intensities of these two gel shift complexes, seen after transfection of E2F-1 alone (Fig. 3A), as if each was the product of an E2F-1–DP-1 (or its equivalent) heterodimer. The faster migrating species is a form of free E2F (*9*). The slower migrating species was disrupted by wild-type E1A, but not by a CR2 mutant unable to bind to the pocket of Rb family members (*10*). Because this complex did not react with antibodies to Rb and p107 (*10*), this E2F-1–DP-1 complex probably contains an E1A binding protein (or proteins) that is related to Rb and p107.

Fig. 2. The E2F-1 zipper is involved in E2F-1–DP-1 heterodimer formation. (**A**) The DNA binding region of E2F-1. (**B**) The IVT product of the b–H1-H2–Zip region of E2F-1 was tested for DNA binding before (lane 6) and after mixing with HA–DP-1 (lane 7). HA mAb supershifting (lane 8) and oligonucleotide competition experiments (lanes 10 and 11) were done as described in Fig. 1B. Arrows indicate the position of complexes A and B. (**C**) As in Fig. 2B, except that the b–H1-H2 region of E2F-1 was assayed. The arrow indicates the position of complex C. (**D**) The b–H1-H2 IVT product was assayed for DNA binding before (lane 2) and after mixing with full-length HA–E2F-1 (lane 3) and the b–H1-H2–Zip segment (lane 7). HA mAb supershifting and oligonucleotide competitions were done as described in Fig. 1C. The arrows indicate the position of specific complexes B, C, Y, and Z.

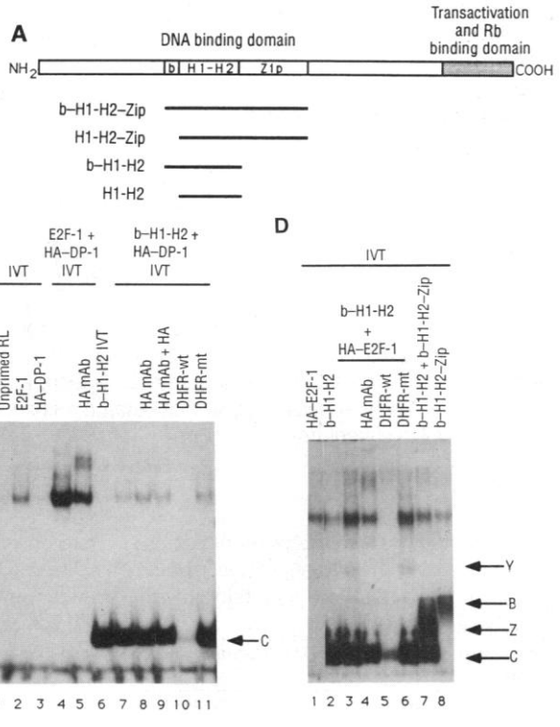

Cotransfection of Rb with HA–E2F-1 resulted in a gel shift complex that comigrated with the Rb-E2F complex from whole-cell extracts (Fig. 3A). The same complex was detected after cotransfection of HA–E2F-1 (or E2F-1), DP-1 (or HA–DP-1), and Rb (Fig. 3A), implying that Rb-E2F complexes contain, at least, Rb, an E2F-1–like subunit, and a DP-1–like subunit, with the latter two present as a heterodimer. Moreover, antibody supershift experiments suggest that E2F-1, DP-1, and Rb exist in the same DNA binding complex in vivo (Fig. 3B). No free E2F was detected (Fig. 3A), implying that heterodimer formation facilitated Rb binding. Competition experiments indicated that the observed DNA binding activities were E2F-specific, and immunoblotting confirmed the presence of HA–E2F-1, HA–DP-1, and E2F-1 (*10*).

After cotransfection of E2F-1 and DP-1 into the Rb (+/+) cell line, U-2 OS, E2F-1–DP-1 complexes formed and were much more active in gel shift assays than either protein alone (Fig. 3C). Only a small fraction of the E2F-1–DP-1 complexes migrated more slowly than known species of free E2F (Fig. 3C). In contrast, transfection of HA–E2F-1 alone led to the appearance of a single complex (Fig. 3C) which resembled that of an endogenous Rb-E2F complex. It was supershifted by HA mAb and by mAbs to Rb (*10*). Transfection of HA–DP-1 alone led to very little DNA binding activity (Fig. 3C), implying that the synthesis or availability of E2F-1 or other suitable E2F family partners may be a limiting factor in the formation of E2F-1–DP-1 heterooligomers in vivo. Together, these results indicate that cosynthesis of E2F-1 and DP-1 results in heterooligomer formation, marked enhancement in their respective DNA binding activities, and efficient complex formation with one or more pocket proteins.

Next, we tested DP-1 for its ability to bind to Rb. When in vitro–translated E2F-1 or DP-1 was mixed with glutathione-S-transferase (GST)–Rb fusion proteins, E2F-1 bound efficiently whereas DP-1 did not (*10*). Similar mixing experiments with in vitro–translated Rb and HA–DP-1 or HA–E2F-1 that were followed by HA mAb immunoprecipitations, indicated that Rb did not bind to HA–DP-1 and bound inefficiently to HA–E2F-1 (Fig. 4A). When all three proteins were mixed, Rb binding was increased (Fig. 4A), indicating that heterodimer formation had facilitated pocket protein binding. Binding of the Rb pocket by E2F-1 is required, because there was no cooperation between DP-1 and an E2F-1 mutant (Δ18) unable to bind to the Rb pocket (Fig. 4A) (*11*). Complexes between this mutant and DP-1 did form (Fig. 4A) and displayed abundant DNA binding activity (*10*).

To test whether DP-1–E2F-1 complex for-

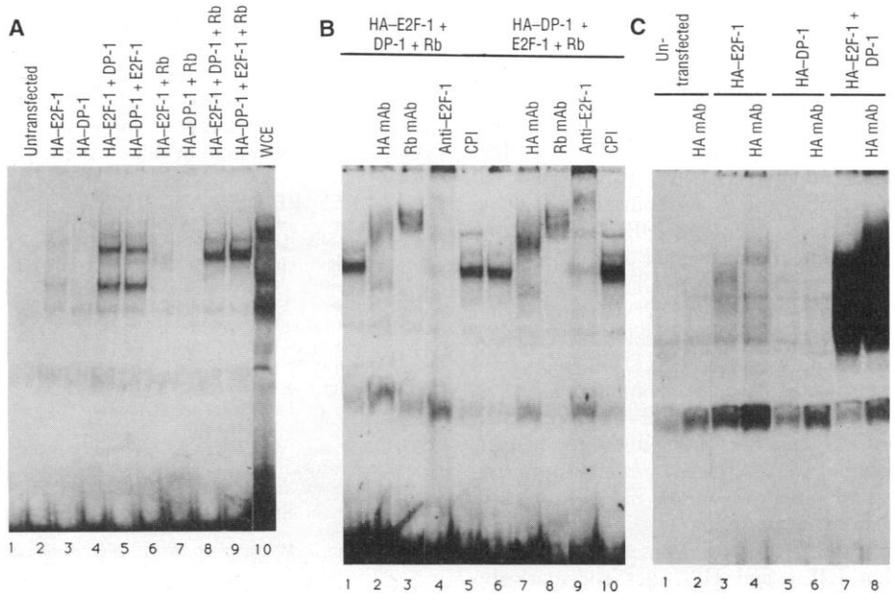

Fig. 3. E2F-1 and DP-1 associate with Rb in vivo and stimulate DNA binding activity. (**A**) Saos-2 (Rb−/−) cells were transfected (*25*) with mammalian expression plasmids as indicated. Extracts were assayed for DNA binding activity (lanes 1 through 9) (*9*). Lane 10 shows cellular E2F complexes (the Rb-E2F complex is underrepresented). (**B**) Extracts of Saos-2 cells transfected with the indicated plasmids were assayed for DNA binding in the absence (lanes 1 and 6) and presence of HA mAb (lanes 2 and 7), RB mAb (mAb C36, lanes 3 and 8), affinity-purified anti–E2F-1 (lanes 4 and 9) (*26*), and corresponding preimmune serum (CPI, lanes 5 and 10). (**C**) U-2 OS cells were transfected with expression plasmids as indicated and assayed for DNA binding. HA mAb supershifting is shown in lanes 2, 4, 6, and 8.

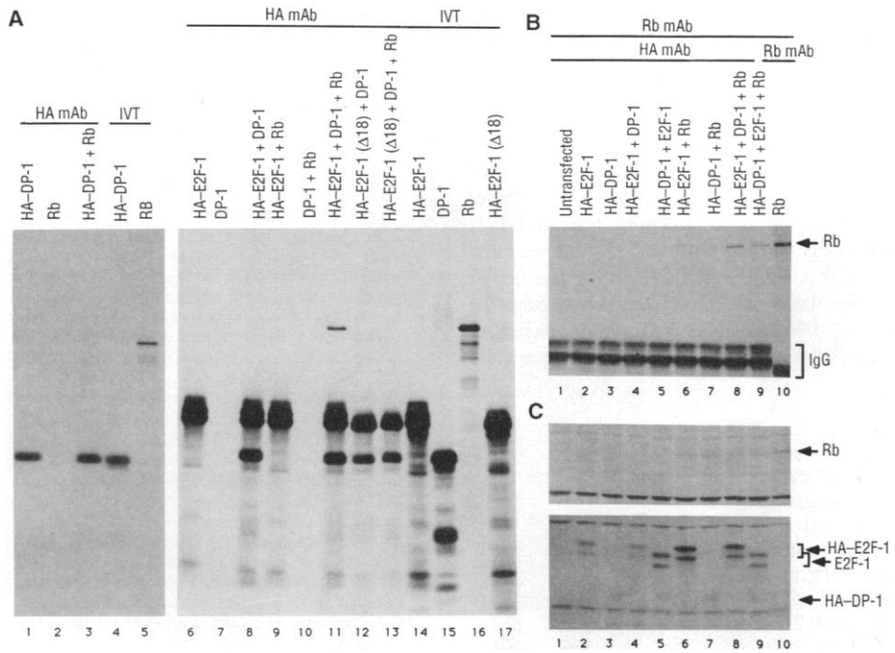

Fig. 4. DP-1 facilitates E2F-1–Rb binding in vitro and in vivo. (**A**) IVT products of E2F-1, DP-1, and Rb, alone or after mixing, were immunoprecipitated with HA mAb (lanes 1 through 3 and 6 through 13) (*23*). IVT products are shown in lanes 4, 5, and 14 through 17. (**B**) Saos-2 cells were transfected with the indicated expression plasmids (lanes 1 through 10). Immunoprecipitations (*23*) were done with either HA mAb (lanes 1 through 9) or RB mAb (XZ77, lane 10). Immunoprecipitates were processed for Western blotting with RB mAb (mAb 245) (*18*). The arrow points to coimmunoprecipitated Rb. (**C**) Aliquots from cell extracts prepared in (B) were immunoblotted with mAb 245 (upper panel), E2F-1 mAb (mAb SQ41) and HA mAb (lower panel) as described (*18*). Arrows indicate the position of the synthesized proteins.

mation facilitates Rb binding in vivo, we transfected Saos-2 cells with different combinations of expression plasmids encoding E2F-1, DP-1, and Rb. The amount of Rb coprecipitating with HA–E2F-1 was significantly increased in the presence of DP-1 (Fig. 4B). Rb did not coprecipitate with HA–DP-1 but bound efficiently when both HA–DP-1 and E2F-1 were present (Fig. 4B). The fact that Rb coimmunoprecipitated with HA–E2F-1 suggests that endogenous DP-1 is available for complex formation with E2F-1 (Fig. 3, A and C). As assessed by immunoblotting (Fig. 4C), the amount of transfected cDNA product was comparable in each reaction mixture.

As shown in Fig. 5, E2F-1 transactivated an E2F reporter plasmid 6- to 10-fold, whereas DP-1 displayed minimal transactivation function. When E2F-1 and DP-1 were cotransfected, a 9- to 17-fold increase in transactivation was observed, suggesting that E2F-1 and DP-1 act cooperatively. Transactivation was dependent on functional E2F sites in the reporter plasmid (*8*).

Existing evidence correlates Rb-dependent G1 blockade with E2F binding (*12*, *13*). Moreover, Rb suppresses the transactivating function of E2F in general (*2*) and of E2F-1 in particular (*14*, *15*). E2F-1 and DP-1 were detected in previously characterized Rb-E2F complexes, which exist in G1 and likely contain unphosphorylated Rb (*9*). Here we show that E2F-1 and DP-1 are bound to one another in that setting as a heterodimeric complex. Because DP-1–E2F-1 heterodimer formation stimulates critical E2F functions, DNA binding, and transactivation, the linked facilitation of Rb binding may be necessary to regulate the ultimate effect of this functional enhancement—activation of certain genes needed for G1 exit or S phase progression or both. Therefore, because DP-1 heterooligomerizes with E2F-1 and recruits Rb, it is possible that DP-1 serves as a negative regulator of G1 exit, until this effect is cancelled by subsequent Rb phosphorylation (*16*). At that point, DP-1 becomes a positive regulator by enhancing the DNA binding activity and transactivation power of the DP-1–E2F-1 oligomer. One might speculate that a positive regulatory effect of DP-1 develops close to or at a decision point in G1 when a cell becomes committed to cell cycle entry.

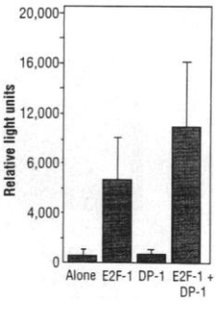

Fig. 5. E2F-1 and DP-1 cooperate in E2F-dependent transactivation. U-2 OS cells were transfected (*25*) with an E2F luciferase reporter plasmid (3xWT E2F-Luc) (*27*) either alone, with E2F-1, with DP-1, or with both E2F-1 and DP-1 (from left to right). The luciferase values were normalized to β-galactosidase units to control for variations in transfection efficiency. The results shown represent three separate experiments and the vertical lines indicate the standard deviations. Similar results were obtained in Saos-2 cells (*8*).

REFERENCES AND NOTES

1. J. Lees *et al.*, *Mol. Cell. Biol.*, in press; D. Ginsberg, T. Chittenden, G. Vairo, D. M. Livingston, unpublished results.
2. J. R. Nevins, *Science* **258**, 424 (1992).
3. W. G. Kaelin *et al.*, *Cell* **70**, 351 (1992).
4. K. Helin *et al.*, *ibid.*, p. 337.
5. B. Shan *et al.*, *Mol. Cell. Biol.* **12**, 5620 (1992).
6. R. Girling *et al.*, *Nature* **362**, 83 (1993).
7. H. E. Huber *et al.*, *Proc. Natl. Acad. Sci. U.S.A.* **90**, 35 (1993).
8. S. Shirodkar, W. Krek, D. M. Livingston, unpublished results.
9. S. Shirodkar *et al.*, *Cell* **68**, 157 (1992).
10. W. Krek, S. Shirodkar, D. M. Livingston, unpublished results.
11. X.-Q. Qin, D. M. Livingston, W. G. Kaelin, in preparation.
12. X.-Q. Qin, T. Chittenden, D. M. Livingston, W. G. Kaelin, *Genes Dev.* **6**, 953 (1992).
13. S. W. Hiebert, *Mol. Cell. Biol.* **13**, 3384 (1993).
14. E. K. Flemington, S. H. Speck, W. G. Kaelin, *Proc. Natl. Acad. Sci. U.S.A.* **90**, 6914 (1993).
15. K. Helin, E. Harlow, A. Fattaey, *Mol. Cell. Biol.* **13**, 6501 (1993).
16. J. A. DeCaprio, Y. Furukawa, F. Ajchenbaum, J. Griffen, D. M. Livingston, *Proc. Natl. Acad. Sci. U.S.A.* **89**, 1795 (1992); J. W. Ludlow, J. Shon, J. M. Pipas, D. M. Livingston, J. A. DeCaprio, *Cell* **60**, 387 (1990); J. A. DeCaprio *et al.*, *ibid.* **58**, 1085 (1989); K. Buchkovich, L. A. Duffy, E. Harlow, *ibid.*, p. 1097; P. Chen, P. Scully, J. Shew, J. Y. J. Wang, W. Lee, *ibid.*, p. 1193; K. Mihara *et al.*, *Science* **246**, 1300 (1989).
17. Q. Hu *et al.*, *Mol. Cell. Biol.* **11**, 5792 (1991).
18. J. A. DeCaprio *et al.*, *Cell* **54**, 275 (1988).
19. C. Chen and H. Okayama, *Mol. Cell. Biol.* **7**, 2745 (1987).
20. F. M. Ausubel *et al.*, *Current Protocols in Molecular Biology* (Green/Wiley-Interscience, New York, 1990) vol. 1.
21. W. Krek, G. Maridor, E. A. Nigg, *J. Cell. Biol.* **116**, 43 (1992).
22. To generate pcDNAI(E2F-1), we cloned the E2F-1 cDNA (excised from pSP72–E2F-1) into pcDNAI-Amp (Invitrogen). A murine DP-1 cDNA clone was used in polymerase chain reactions (PCR) for the generation of a wild-type clone, which was confirmed by DNA sequencing. We generated pcDNAI(DP-1) by cloning the wild-type DP-1 cDNA into pcDNAIAmp and constructed pcDNAI(HA–E2F-1) and pcDNAI(HA–DP-1) by cloning NH_2-terminal to the cDNA an oligonucleotide encoding the HA epitope (5′-AGCTTACCATGGCCTACCCCTACGACGTGCCCGACTACGCCTCCCTCG-3′ and 5′-GATCCGAGGGAGGCGTAGTCGGGCACGTCGTAGGGGTAGGCCATGGTA-3′). The construct pcDNAI(HA–E2F-1Δ18) was created by cloning the mutated E2F-1 cDNA from pSG5–E2F-1(Δ18) [described elsewhere (*11*)] into pcDNAIAmp. E2F-1 derivatives [b–H1-H2–Zip (residues 102 to 241), H1-H2–Zip (residues 128 to 241), b–H1-H2 (residues 102 to 196), and H1-H2 (residues 128 to 196)] were constructed by one-step PCR reactions and verified by DNA sequencing.
23. The ^{35}S-labeled in vitro translation (IVT) products were prepared with the TNT lysate system (Promega), according to manufacturer's instructions. For coimmunoprecipitations, 4 μl of each IVT product (unless otherwise specified) was mixed with 200 μl of buffer A [50 mM KCl, 20 mM Hepes (pH 7.5), 10 mM $MgCl_2$, 10% glycerol, 0.5 mM dithiothreitol (DTT), 0.1% NP-40, aprotinin (1 mg/ml), and 1 mM phenylmethylsulfonyl fluoride (PMSF)], incubated for 30 min at room temperature, and then rocked for 30 min at 4°C. Then, 800 μl of TNN buffer [50 mM tris (pH 7.4), 150 mM NaCl, 5 mM EDTA, 0.5% NP-40, 50 mM NaF, 0.2 mM Na_3VO_4, 1 mM DTT, aprotinin (1 mg/ml), and 1 mM PMSF] was added. Affinity-purified HA mAb (0.5 μl, mAb 12CA5; BAbCo) was added and the mixture rocked at 4°C for 30 min. Subsequently, 60 μl of a 50% (w/v) slurry of protein A–Sepharose beads (Pharmacia) was added and the mixture rocked for 30 min at 4°C and then washed five times in TNN buffer. Immunobeads were boiled in sample buffer and the products analyzed electrophoretically. Transfected cells were washed twice with cold phosphate-buffered saline (PBS), lysed for 30 min on ice in 500 μl of TNN buffer, and immunoprecipitated with either 1 μl of HA mAb or 50 μl of tissue culture supernatant of XZ77 (Rb mAb) (*17*). Immunoblotting was as described (*18*) with equal amounts of the above TNN extract.
24. Binding reactions for electrophoretic mobility-shift assays (EMSAs) were done with 1 μl of each IVT product and incubated in 20 μl of gel shift buffer (*9*) for 20 min at 25°C. For antibody supershifts, 1 μl of affinity-purified HA mAb was added and incubated at 25°C for an additional 20 min. For peptide competition experiments, 1 μl of affinity-purified HA mAb was preincubated with 4 μg of HA peptide (BAbCo), and 1 μl of this mixture was used in supershift experiments. EMSA was done as described (*9*).
25. Saos-2 and U-2 OS cells were grown as described (*12*) and transfected on 10-cm dishes for 16 hours by the calcium-phosphate method (*19*). Transfections included 8 μg of expression plasmids encoding HA–E2F-1, E2F-1, HA–DP-1, and DP-1 and, where indicated, 25 μg of Rb expression plasmid or vector control. For transactivation studies, the following quantities of DNA were used: 10 μg of reporter plasmid, 2 μg of E2F-1–DP-1 cDNAs (when each was transfected alone) or 2 μg of E2F-1 and 0.5 μg of DP-1 (when cotransfected), 2 μg of pCMVβgal, and pBSSK-II (Stratagene) to a total of 20 μg. Transfected cells were washed twice with PBS and fed again with growth medium. We prepared the extracts 24 hours after removal of the precipitate. Cells were washed twice with PBS and lysed in 60 μl of extract buffer (EB) [20 mM Hepes (pH 7.9), 1 mM EDTA, 0.4 M NaCl, 25% glycerol, 2.5 mM DTT, 5 mM NaF, 0.5 mM Na_3VO_4, 0.1% NP-40, 0.5 mM PMSF, and aprotinin (1 μg/μl) for 30 min on ice. Extracts were clarified by centrifugation, quantitated with the BioRad protein assay kit, and used directly for EMSA (2 μl per assay). Luciferase and β-galactosidase (*20*) assays were done as described.
26. Polyclonal rabbit serum to E2F-1 (anti–E2F-1) was raised against a GST–E2F-1 fusion protein (p98 serum) (*3*), and it was affinity purified by incubation first with a GST affinity column and then with a GST–E2F-1 fusion protein affinity column, which we prepared by covalently cross-linking the relevant proteins to gluthathione-Sepharose with dimethyl pimelimidate (Pierce). Incubation and elution of antibodies were as described (*21*).
27. To construct 3xWTLuc (and 3xMUTLuc) we cloned two oligonucleotides, one bearing a TATA box and the other containing three E2F wild-type (or mutant) sites, into pGL2BASIC (Promega) and validated it by DNA sequencing. TATA oligonucleotide: 5′-GATCTACTTGGGCATAAAAGGCAGAGCAGGGCAGCTGCTGCTTACACTTA-3′; 3xE2F WT oligonucleotide: 5′-CTGCAATTTCGCGCCAAACTTGTGCAATTTCGCGCCAAACTTGTGCAATTTCGCGCCAAACTTGC-3′; and 3xE2F MUT oligonucleotide: 5′-CTGCAATTGCTCGACCAACTTGTGCAATTGCTCGACCAACTTGTGCAATTGCTCGACCAACTTGC-3′.

28. We thank the members of our division for helpful discussions; W. Kaelin for the E2F-1 cDNA and E2F-1 serum; J. DeCaprio for the mAb SQ41; E. Harlow for the mAb XZ77; and R. Girling and N. B. La Thangue (Medical Research Council, London) for the murine DP-1 cDNA clone. S.S. is the Sharf-Green Family Fellow of the Dana-Farber Cancer Institute and W.K. was supported by a fellowship from the European Molecular Biology Organization. Supported by grants from The National Institutes of Health.

15 July 1993; accepted 15 October 1993